Superweak momentum transfer near optical vortices

Stephen M Barnett[1] & M V Berry[2]

[1] Department of Physics, University of Strathclyde, Glasgow G4 0NG, UK

[2] H H Wills Physics Laboratory, Tyndall Avenue, Bristol BS8 1TL, UK

Abstract

Near a vortex in a monochromatic light beam, the length of the local wavevector (phase gradient) can exceed the wavenumber in any of the plane waves in the superposition representing the beam. One way to detect these 'superweak' momenta could be by 'superkicks' imparted to a small particle located near the vortex, by absorbing individual large-momentum photons from the beam. A model for this process is a two-level atom with a transition resonant with the light beam. A semiclassical analysis shows that the momentum distribution of the atom is shifted by interaction with the vortex beam, by amounts less than the target superkicks but greater than the momenta in the plane waves comprising the beam.

1 Introduction

A fundamental feature of phase singularities [1-4] of monochromatic fields representing waves in three-dimensional space r is that they are optical vortex lines, near which the phase varies on scales smaller than the wavelength λ. It follows that the length of the local wavevector $k(r)$ – the phase gradient – exceeds the free-space wavenumber $k_0 = 2\pi/\lambda$. Such rapid variations are now recognized as 'superoscillations'[5, 6], where the 'weak value' [7] of momentum $\hbar k(r)$ exceeds the free-space momentum $\hbar k_0$. The question we address here, in the spirit of quantum weak measurement theory [8-10], is whether such large local momenta could be imparted as 'superkicks' to test particles ('atoms') in the field. This situation appears paradoxical, because the momentum $\hbar k(r)$ imparted to the absorbing particle exceeds that of any single photon in the field, raising concerns about global momentum conservation. Our resolution follows from considering the quantum mechanics of the motion of an absorbing atom. We need to account for the wave nature both of the electromagnetic field and the atom used to probe it.

A local model for the field strength near a vortex line of strength m on the z axis of a linearly polarized paraxial wave, is

$$
\begin{aligned}
&E_m(r,t) = E_m(r)\exp(-i\omega t), \quad \omega = ck_0, \\
&E_m(r) = Nr^m \exp\{i(m\phi + k_0 z)\} = N(x+iy)^m \exp(ik_0 z),
\end{aligned}
\tag{1.1}
$$

in which here and hereafter N denotes a generic multiplier or normalization constant. The corresponding local wavevector is

$$
k(r) = \nabla \arg E_m(r,t) = \frac{m}{r}e_\phi + k_0 e_z.
\tag{1.2}
$$

Its transverse part exceeds k_0 inside the cylinder $k_0 r < m$. The factor $(x+\mathrm{i}y)^m$ describes any locally symmetric vortex on strength m; it is also a small-r approximation to the exact Bessel beam solution [11] of the Helmholtz equation:

$$E_{m,\text{Bessel}}(\boldsymbol{r}) = N J_m(Kr)\exp\left\{\mathrm{i}\left(m\phi + z\sqrt{k_0^2 - K^2} - \omega t\right)\right\}. \qquad (1.3)$$

Paraxiality corresponds to $K \ll k_0$.

In section 2 we derive the approximate Hamiltonian for a model quantum detector in the form of a two-level atom placed in the field, and show that when the atom gets excited its position wavefunction inherits the form of the optical field. In section 3 we calculate the corresponding atomic momentum distribution, incorporating the momentum uncertainty implied by localizing the atom near the vortex. In particular, we calculate the average momentum, and elucidate the conditions under which this can exceed the momentum of free-space optical photons.

This study, developing an idea envisaged earlier [7, 12], complements and extends existing explorations [13, 14] of possible quantum effects associated with the cores of optical vortices.

2. Atom Hamiltonian

As a probe for the optical field, we consider a model two-level atom of mass M, with electronic ground and excited states $|g\rangle$ and $|e\rangle$ and corresponding energies ε_g and ε_e, coupled by electric dipole interaction. It suffices to work within the semi-classical approximation, in which the atom is treated quantum mechanically and the field is described

3

classically [15, 16]. We can describe the coupled the atom-field system
by the state $|\Psi_0(t)\rangle$, driven by the Hamiltonian

$$\hat{H}_0 = \frac{\hat{p}^2}{2M} + \varepsilon_e |e\rangle\langle e| + \varepsilon_g |g\rangle\langle g| - \hat{\mu}\left[E_m(\boldsymbol{r},t) + E_m^*(\boldsymbol{r},t)\right], \qquad (2.1)$$

where $\hat{p}^2$ is the square of the total atomic momentum and $\hat{\mu}$ is the
electric dipole operator. Neither of the electronic states has an intrinsic
dipole moment, so the dipole operator has only off-diagonal matrix
elements in this basis and can be written in the form

$$\hat{\mu} = \mu\left(|g\rangle\langle e| + |e\rangle\langle g|\right) . \qquad (2.2)$$

We immediately eliminate some of the fast oscillations by
transforming to a new state $|\Psi(t)\rangle$ (equivalent to the interaction picture):

$$|\Psi_0(t)\rangle = \exp\left\{-\frac{i}{\hbar}t\left(\varepsilon_g|g\rangle\langle g| + \varepsilon_e|e\rangle\langle e|\right)\right\}|\Psi(t)\rangle. \qquad (2.4)$$

Thus the Schrödinger equation is

$$i\hbar\partial_t|\Psi(t)\rangle = \hat{H}|\Psi(t)\rangle. \qquad (2.5)$$

with the new Hamiltonian

$$\hat{H} = \frac{\hat{p}^2}{2M} - \mu\left(|g\rangle\langle e|\exp\left\{-\frac{i}{\hbar}(\varepsilon_e - \varepsilon_g)\right\} + \right.$$
$$\left. + |e\rangle\langle g|\exp\left\{\frac{i}{\hbar}(\varepsilon_e - \varepsilon_g)\right\}\right)\left(E_m(\boldsymbol{r},t) + E_m^*(\boldsymbol{r},t)\right). \qquad (2.6)$$

(Here we have used the fact that $|g\rangle$ and $|e\rangle$ are orthogonal, and the
consequence that the operators $|e\rangle\langle e|$ and $|g\rangle\langle g|$ commute.)

We can make three further simplifications. First we can make the atom sufficiently massive and slowly-moving such that the first (kinetic) term has little effect during the short times will be of interest to us and can be neglected. Second, we choose exact resonance, so that $\varepsilon_e - \varepsilon_g = \hbar\omega$. Third, we note that from the form of the electric field amplitude (1.1), $\hat{H}$ contains time-independent terms and also terms rotating at 2ω: twice the optical frequency. The effect of these rapidly rotating terms will tend to average out over relevant time scales, and discarding them leads to the final time-independent 'rotating wave' Hamiltonian [16]:

$$\hat{H}_{RW} = -\mu\left(\,|g\rangle\langle e|\,E_m^*(\boldsymbol{r}) + |e\rangle\langle g|\,E_m(\boldsymbol{r})\right) \,, \tag{2.7}$$

We can now analyse the effect on the atomic motion of absorbing a quantum of energy near to the vortex core, where the local optical momentum $|\boldsymbol{k}(\boldsymbol{r})| > k_0$. In doing so it is essential to include a quantum description of the motional state of the atom as well as its electronic state.

Let the initial state of the atom be

$$\langle\boldsymbol{r}|\Psi(0)\rangle = |g\rangle\psi_{\text{init}}(\boldsymbol{r}) \,, \tag{2.8}$$

corresponding to the atom being in its electronic ground state and in the motional state $\psi_{\text{init}}(\boldsymbol{r})$. After a short time this state will evolve to a superposition of the ground and excited states. We can describe this using first-order perturbation theory, because we are interested only in the effects of a single absorption event.

$$\langle r | \Psi(t) \rangle \approx \left(1 - i \frac{\hat{H}_{RW} t}{\hbar} \right) \langle r | \Psi(0) \rangle$$

$$= |g\rangle \psi_{\text{init}}(r) - i \frac{\mu t}{\hbar} E_m(r) |e\rangle \psi_{\text{init}}(r) . \tag{2.9}$$

If after this short time the atom has made a transition to the excited state (by absorbing a single quantum from the field) then its associated motional wavefunction will be

$$\psi_m(r) = N(x + iy)^m \exp(ik_0 z) \psi_{\text{init}}(r) , \tag{2.10}$$

Clearly, the phase of the electric field has been imprinted on the motional wavefunction and this encodes the 'kick' given to the atom. Our focus will be on the transverse momentum, but we note the immediate obvious consequence of (2.10) that for $\psi_m(r)$ the average momentum in the z-direction exceeds by $\hbar k_0$ that for $\psi_{\text{init}}(r)$. This is the familiar atomic recoil associated with the conservation of linear momentum.

3. Momentum distribution

It follows from (2.10) that the momentum state of the excited atom is given in terms of the initial momentum state $\bar{\psi}_0(k)$ (Fourier transform of (2.10)) by

$$\bar{\psi}_m(k) = N\left(\partial_{k_x} + i\partial_{k_y} \right)^m \bar{\psi}_{\text{init}}\left(k_x, k_y, k_z - k_0 \right). \tag{3.1}$$

An immediate consequence is that the final momentum state can contain only momenta that were present in the initial state: the only effect of the interaction with the light is a redistribution of momenta that the atom already possessed as a result of its localization near the vortex. In

particular, if the initial momentum state has bounded support in k, the final state has the same bounded support.

Nevertheless, it is possible for the atom to acquire momenta larger than k_0. We explore this for an initial (unexcited) atomic wavefunction located close to $r=(x_0,0,0)$, in the form of the Gaussian

$$\psi_{\text{init}}(r) = N \exp\left(-\frac{(x-x_0)^2 + y^2 + z^2}{2\sigma^2}\right), \tag{3.2}$$

In order to localize the atom in the region $k_0 r < m$ where the light is superoscillatory, we restrict the position x_0 and the width σ to

$$x_0 < \frac{m}{k_0} = \frac{2\pi m}{\lambda}, \quad \sigma < m\lambda . \tag{3.3}$$

The corresponding initial momentum distribution is

$$\bar{\psi}_{\text{init}}(k) = N \exp\left(-\tfrac{1}{2}\sigma^2\left(k_x^2 + k_y^2 + k_z^2\right) + ik_x x_0\right). \tag{3.4}$$

An easy calculation (iterating (3.1) for successive values of m) gives the final momentum probability distribution

$$\left|\bar{\psi}_m(k)\right|^2 = N^2 \exp\left(-\left(k_z - k_0\right)^2 \sigma^2\right) \times$$
$$\left(k_x^2 + \left(k_y + x_0/\sigma^2\right)^2\right)^m \exp\left(-\left(k_x^2 + k_y^2\right)\sigma^2\right). \tag{3.5}$$

This shows that in addition to the obvious z momentum shift by k_0, the distribution is skewed towards $+y$ (if $x_0 > 0$), as illustrated in figure 1 for several values of x_0/σ and m.

To quantify this y kick, we calculate the momentum expectation values for different vortex strengths m:

7

$$\langle \boldsymbol{k}_m \rangle = \frac{\iint \mathrm{d}\boldsymbol{k}\, \boldsymbol{k} \left| \bar{\psi}_m(\boldsymbol{k}) \right|^2}{\iint \mathrm{d}\boldsymbol{k} \left| \bar{\psi}_m(\boldsymbol{k}) \right|^2} \equiv k_m \boldsymbol{e}_y + k_0 \boldsymbol{e}_z \ . \tag{3.6}$$

The k_y shifts can be evaluated exactly in terms of Laguerre polynomials [17]:

$$k_m = \frac{x_0 L_{m-1}^{(1)}\left(-x_0^2/\sigma^2\right)}{\sigma^2 L_m\left(-x_0^2/\sigma^2\right)} = \frac{1}{2}\partial_{x_0} \log\left(L_m\left(-x_0^2/\sigma^2\right)\right). \tag{3.7}$$

The first few shifts are

$$k_1 = \frac{x_0}{\sigma^2 + x_0^2}, \quad k_2 = \frac{2x_0\left(2\sigma^2 + x_0^2\right)}{2\sigma^4 + 4x_0^2\sigma^2 + x_0^4},$$

$$k_3 = \frac{3x_0\left(6\sigma^4 + 6x_0^2\sigma^2 + x_0^4\right)}{6\sigma^6 + 18x_0^2\sigma^4 + 9x_0^4\sigma^2 + x_0^6}, \tag{3.8}$$

$$k_4 = \frac{4x_0\left(24\sigma^6 + x_0^2\left(6\sigma^2 + x_0^2\right)^2\right)}{24\sigma^8 + 96x_0^2\sigma^6 + 72x_0^4\sigma^4 + 16x_0^6\sigma^2 + x_0^8}.$$

These functions should be compared with the corresponding superkicks that we hope to detect in the optical field, given by (cf. (1.2))

$$k_{m,\text{super}} = \frac{m}{x_0} \ . \tag{3.9}$$

Comparisons are shown in figure 2. The average momentum shifts acquired by the atoms reach their greatest value $k_{m\max}$ when $x_0 = x_{0\max} \sim \sigma$; the precise values are given in Table 1.

m	1	2	3	4	5	6
$x_{0\max}/\sigma$	1	0.939	0.900	0.874	0.854	0.840
$k_{m\max}\sigma$	0.5	0.858	1.151	1.404	1.629	1.835

Table 1. Maximal momentum shifts for vortex strengths m

Figure 3 shows the momentum distributions along the symmetry line $k_x=0$ for x_0 corresponding to these maximum shifts, illustrating how the shifts get bigger for larger m.

It is clear from figure 2 that the average momentum shifts tend to the superkick values (3.9) as x_0 increases but fall short for smaller x_0. The shifts vanish as $x_o \to 0$, because then the atomic wavefunction overlaps the other side of the vortex where $\boldsymbol{k}(\boldsymbol{r})$ is in the opposite direction. Notwithstanding the shortfall, in the superoscillatory region near the vortex where the the atom shifts are maximal (Table 1) these shifts exceed the momenta k_0 in the plane-wave superpositions comprising the field, by an amount

$$\frac{k_{m\max}}{k_0} = \frac{\left(k_{m\max}\sigma\right)}{2\pi}\frac{\lambda}{\sigma} \sim \frac{\left(k_{m\max}\sigma\right)}{2\pi}\frac{\lambda}{x_o}, \tag{3.10}$$

which is greater than unity if the atom is close enough to the vortex.

We have calculated the momentum distribution of the atom on the assumption that a resonant transition has taken place. However, the probability that such a transition will occur is very small when the atom is near a vortex. From (2.9), standard time-dependent perturbation theory gives the transition probability per unit time as

$$P \propto \int d\boldsymbol{r}\left|\langle \boldsymbol{r}, e | \Psi(t)\rangle\right|^2 \propto N \int d\boldsymbol{r}\left|E_m(\boldsymbol{r})\right|^2\left|\psi_{\text{init}}(\boldsymbol{r})\right|^2$$
$$\approx N\left|E_m(x_0,0,0)\right|^2 = Nx_0^{2m}, \tag{3.11}$$

where we have assumed that ψ_{init} is localized near $(x_0,0,0)$ as in (3.2), and the field has the vortex form (2.1). This is consistent with the following

picture [7, 12] for the time-averaged force on the atom (classical radiation pressure), resulting from the collective effect of many quantum transitions. The force, given by the probability per unit time multiplied by the momentum shift at each transition, is proportional to the large momentum transfer (the superkick) weighted by the weak light intensity. Classically, this corresponds to the important distinction, emphasized earlier [7], between the local momentum $\hbar \mathbf{k}(\mathbf{r})$ and the local current

$$\mathrm{Im}\left[E_m^*(\mathbf{r})\nabla E_m(\mathbf{r})\right]=\left|E_m(\mathbf{r})\right|^2 \mathbf{k}(\mathbf{r}). \tag{3.12}$$

4. Concluding remarks

It is important to consider how superkicks might be observed in an experiment. The natural way to proceed would be to trap a suitable atom and to cool it to its motional ground state. In this state the atomic motional wavefunction will be approximately Gaussian, the width of which will be determined by the experimentally controllable trapping potential. If the trap is switched off then the atomic wave-packet will spread but, for sufficiently short times, the atom will remain localised near to the trap position. Applying a short laser pulse carrying orbital angular momentum will induce a transition to the atomic excited state and with it the superkick of interest. This should be observable by examining the momentum probability distribution for the excited atom.

A number of improvements on this basic idea may make superweak momentum transfer more readily observable. The first is the use of a Bose-Einstein condensate rather than a single atom. Such condensates have the advantage that many atoms share the same motional state; a transition for a small proportion of these may be more readily

observable than a low-probability transition for a single trapped atom. Moreover, the use of a two-photon Raman transition rather than a single-photon transition would make it possible to remove the large momentum kick in the z direction, the existence of which might otherwise mask the azimuthal superkick we seek. Finally, using a magnetic trap may remove the requirement for turning off the trap before applying the electromagnetic field. If the field is tuned so as to flip the electron spin in the trapped atom then the trapping potential will become repulsive and the trapped atom will be ejected from the trap. The superkick should then be visible as a preferred azimuthal direction of ejection from the trap. Assessing which of these ideas provides the greatest potential for observing superweak momentum transfer requires further details of the particular experimental arrangement and lies beyond the scope of this paper.

Finally, we note a curious feature of the classical mechanics of the test particles we have been considering, as represented by the time-averaged force on them, in circumstances where this is proportional to the Poynting vector [7, 18]. For the scalar model we have used here, the time-averaged force is

$$F(r) \propto \left| E_m(r) \right|^2 k(r), \tag{4.1}$$

in which the local wavevector momentum is multiplied by the wave intensity, in contrast with the bare wavevector as in the quantum kicks $\hbar k(r)$. As is known [19, 20] and has been emphasized [21], this force has non-zero curl, so it is not derivable from a potential. In such 'curl forces' [22], the classical motion is Newtonian but not Hamiltonian or Lagrangian, so – for example – Noether's theorem does not apply, and the link between symmetries and conservation laws is broken. It is hard to

see how such non-hamiltonian physics can be directly quantized, but our analysis reported here, in which classical radiation pressure (here associated with a curl force) is quantally deconstructed into individual superkicks, points to a route where quantum effects might nevertheless be understood.

Figure captions

Figure 1. Momentum distribution (3.5) of excited atom in transverse planes, for (a) $x_0=\sigma$, $m=1$, (b) $x_0=\sigma$, $m=3$, (c) $x_0=2\sigma$, $m=3$, (d) $x_0=5\sigma$, $m=4$.

Figure 2. Full curves: mean momentum shifts k_m in y direction (equations (3.6) and (3.7); dashed curves: local optical momenta (target superkicks) $k_{m,\text{super}}$ (equation (3.9)); as functions of the atom position x_0, for (a) $m=1$, (b), $m=2$, (c) $m=3$, (d) $m=4$.

Figure 3. Full curves: momentum distributions (3.4) of the excited atom along the symmetry line $k_x=0$ for fixed k_z, for atom positions x_0 corresponding to the maximum average shifts in Table 1, for (a) $m=1$; (b) $m=3$; (c) $m=5$; (d) $m=7$. Dashed curves: the corresponding initial atomic

momentum distributions (3.4). (The curves are normalized to facilitate comparison.)

References

1. Nye, J. F. & Berry, M. V.,1974, Dislocations in wave trains *Proc. Roy. Soc. Lond.* **A336**, 165-90

2. Nye, J. F.,1999, *Natural focusing and fine structure of light: Caustics and wave dislocations* (Institute of Physics Publishing, Bristol)

3. Dennis, M. R., O'Holleran, K. & Padgett, M. J.,2009, Singular Optics: Optical Vortices and Polarization Singularities *Progress in Optics* **(in press)**

4. Berry, M. V.,1998, Much ado about nothing: optical dislocation lines (phase singularities, zeros, vortices...) *SPIE* **3487**, 1-5

5. Berry, M. V.,1994, *Faster than Fourier in Quantum Coherence and Reality; in celebration of the 60th Birthday of Yakir Aharonov* eds. Anandan, J. S. & Safko, J. L. (World Scientific, Singapore), pp. 55-65.

6. Berry, M. V.,2013, A note on superoscillations associated with Bessel beams *J.Opt.* **15**, 044006 (5pp)

7. Berry, M. V.,2009, Optical currents *J. Opt. A.* **11**, 094001

8. Aharonov, Y., Albert, D. Z. & Vaidman, L.,1988, How the result of a measurement of a component of the spin of a spin 1/2 particle can turn out to be 100 *Phys. Rev. Lett.* **60**, 1351-1354

9. Aharonov, Y. & Rohrlich, D.,2005, *Quantum Paradoxes: Quantum Theory for the perplexed* (Wiley-VCH, Weinheim)

10. Aharonov, Y., Popescu, S. & Tollaksen, J.,2010, A time-symmetric formulation of quantum mechanics *Physics Today* **63**, issue 11, 27-33

11. Durnin, J.,1987, Exact solutions for nondiffracting beams. I. The scalar theory *J. Opt. Soc. Amer.* **4**, 651-654

12. Berry, M. V.,2013, Five momenta *Eur. J. Phys.* **44**, 1337-1348

13. Berry, M. V. & Dennis, M. R.,2004, Quantum cores of optical phase singularities *J.Optics A* **6**, S178-S180

14. Barnett, S. M.,2008, On the quantum core of an optical vortex *J. Mod. Opt.* **55**, 2279-2292

15. Loudon, R.,2000, *The quantum theory of light* (University Press, Oxford)

16. Barnett, S. M. & Radmore, P. M.,1997, *Methods in Theoretical Quantum Optics* (University Press, Oxford)

17. DLMF,2010, *NIST Handbook of Mathematical Functions* (University Press, Cambridge)http://dlmf.nist.gov.

18. Bliokh, K. Y., Bekshaev, A. Y., Kofman, A. G. & Nori, F.,2013, Photon trajectories, anomalous velocities and weak measurements: a classical interpretation *New. J. Phys.* **15**, 073022 (17pp)

19. Ashkin, A. & Gordon, J. P.,1983, Stability of radiation-pressure particle traps: an optical Earnshaw theorem *Opt. Lett.* **8**, 511-513

20. Gómez-Medina, R., Nieto-Vesperinas, M. & Sáenz, J. J.,2011, Nonconservative electric and magnetic optical forces on submicron dielectric particles *Phys. Rev. A* **83**, 033825

21. Berry, M. V. & Shukla, P.,2013, Physical curl forces: dipole dynamics near optical vortices *J. Phys. A (submitted)*

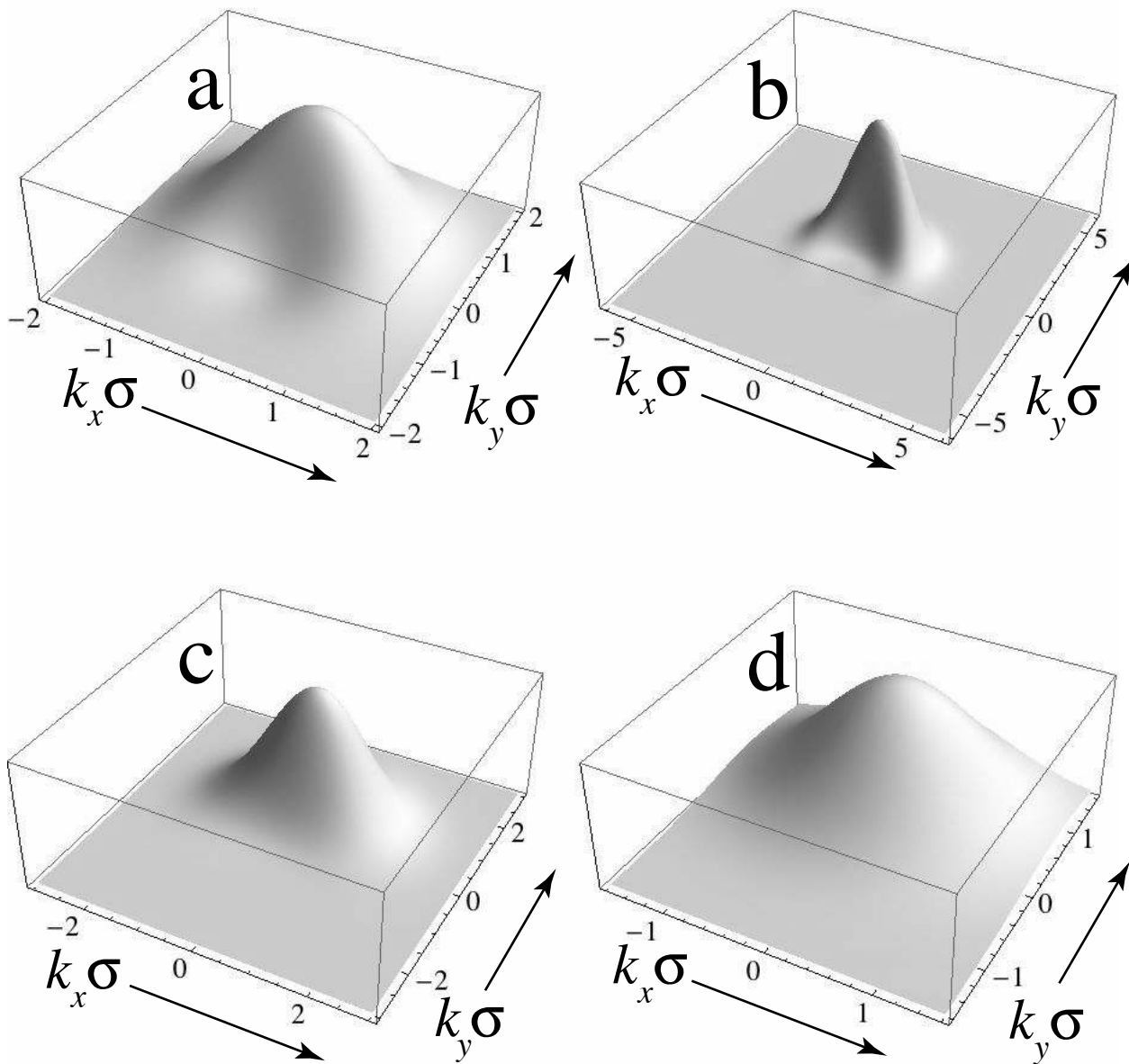22. Berry, M. V. & Shukla, P.,2012, Classical dynamics with curl forces, and motion driven by time-dependent flux *J. Phys. A* **45**, 305201
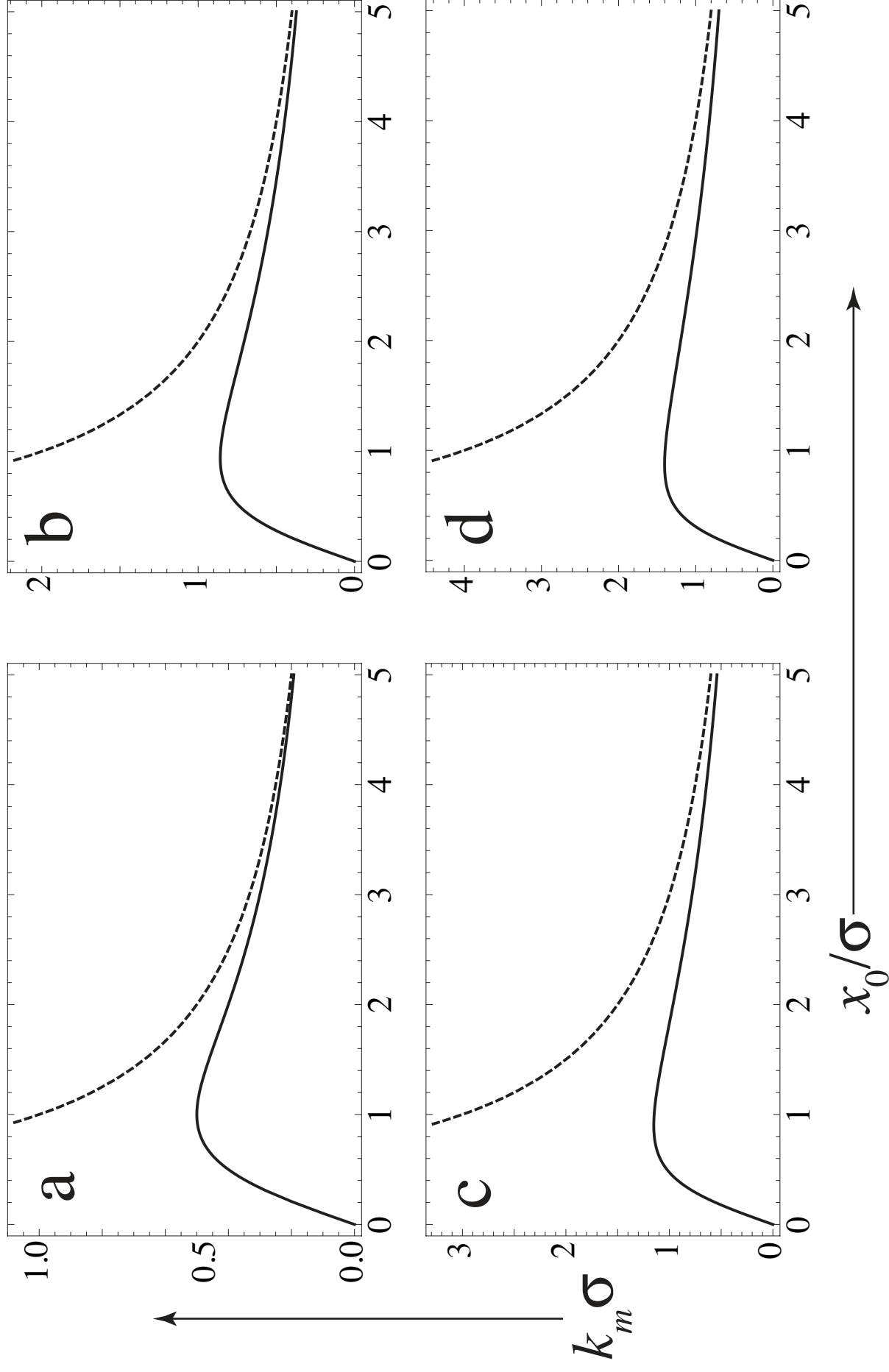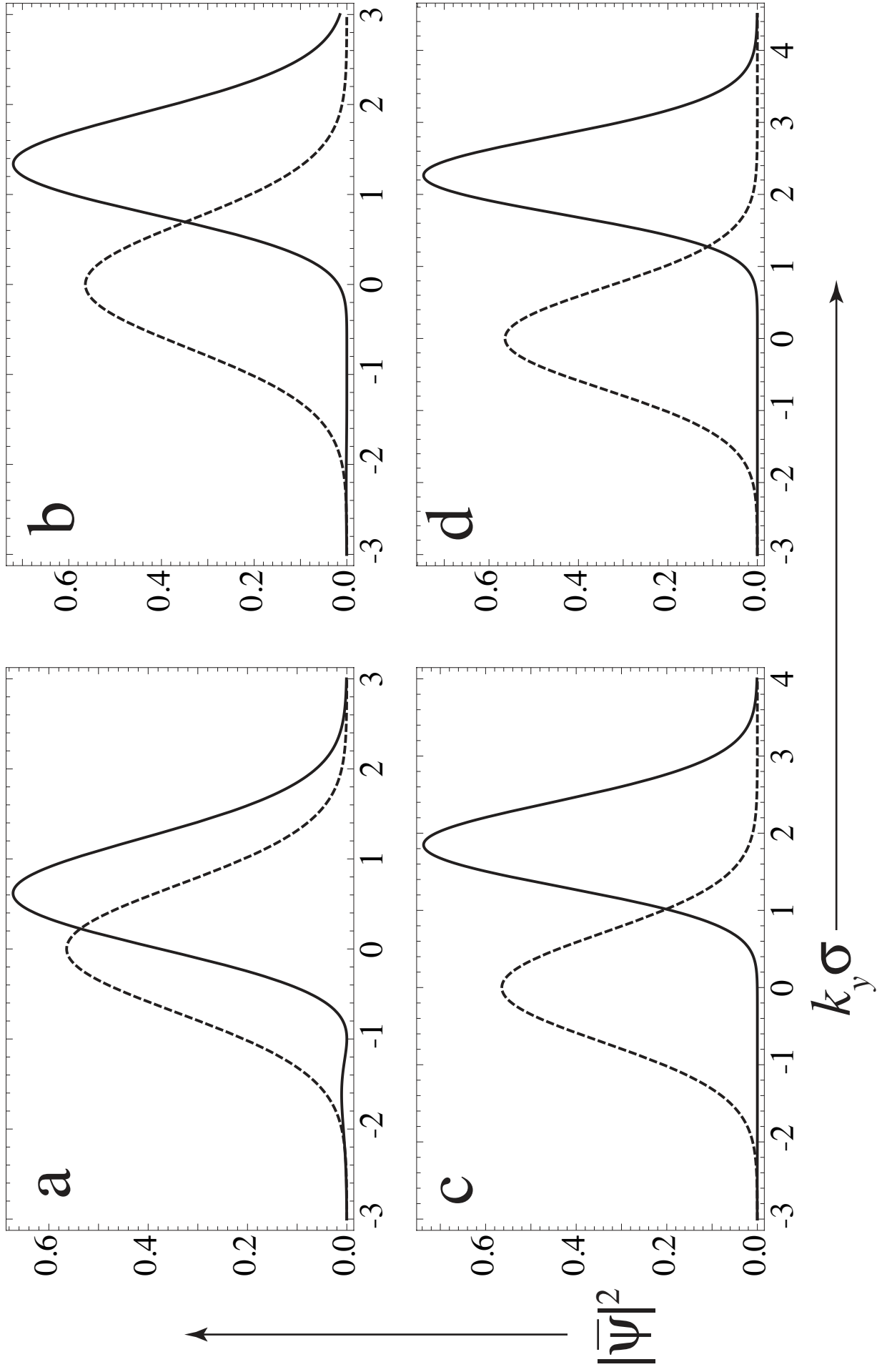
figure 1

figure 2

figure 3